

First numerical results for the reconstruction of velocity profiles of rotating axisymmetric objects

Praveen Kalarickel Ramakrishnan

May 29, 2021

1 Inversion procedure for rotating media

The reconstruction of velocity profiles of moving media using electromagnetic inverse scattering techniques is an important subject. Such techniques have been exploited for axially moving cylinders in [1], [2]. Here we study the reconstruction of the rotating speeds of axisymmetric media, which has numerous practical applications, for example in the tachometry of celestial bodies [3], [4], [5].

The unknown parameters of the inverse scattering problem may be represented by the algebraic vector $\mathbf{u} = (\mathbf{u}_g, \mathbf{u}_d, \mathbf{u}_v) \in \mathbb{R}^{I+J+K}$, where $\mathbf{u}_g \in \mathbb{R}^I$, $\mathbf{u}_d \in \mathbb{R}^J$ and $\mathbf{u}_v \in \mathbb{R}^K$ are respectively the components having the geometric, dielectric and velocity parameters [1].

A set of S plane wave sources illuminate the scatterer. The positions of the sources are denoted by an integer parameter $s = 1, \dots, S$. The electric and magnetic fields are measured using M sensors whose positions are indicated by the parameter $m = 1, \dots, M$. The measured electric and magnetic fields are denoted respectively by $\mathbf{E}^{meas}(s, m, \mathbf{u})$ and $\mathbf{H}^{meas}(s, m, \mathbf{u})$.

For a trial solution $\mathbf{u}^{trial} = (\mathbf{u}_g^{trial}, \mathbf{u}_d^{trial}, \mathbf{u}_v^{trial}) \in \mathbb{R}^{I+J+K}$, we may assume to have a forward scattering procedure (fsp), either semi analytic [4] or numerical [5] that enables us to calculate the fields $\mathbf{E}^{fsp}(s, m, \mathbf{u}^{trial})$ and $\mathbf{H}^{fsp}(s, m, \mathbf{u}^{trial})$.

The above quantities can be used to define the following cost function which is to be minimized using an optimization algorithm to get the best estimate of the unknown parameters.

$$CF(\mathbf{u}, \mathbf{u}^{trial}) = \frac{\sum_{s=1}^S \sum_{m=1}^M \|\mathbf{E}^{fsp}(s, m, \mathbf{u}^{trial}) - \mathbf{E}^{meas}(s, m, \mathbf{u})\|_2^2}{\sum_{s=1}^S \sum_{m=1}^M \|\mathbf{E}^{meas}(s, m, \mathbf{u})\|_2^2} + \frac{\sum_{s=1}^S \sum_{m=1}^M \|\mathbf{H}^{fsp}(s, m, \mathbf{u}^{trial}) - \mathbf{H}^{meas}(s, m, \mathbf{u})\|_2^2}{\sum_{s=1}^S \sum_{m=1}^M \|\mathbf{H}^{meas}(s, m, \mathbf{u})\|_2^2} \quad (1)$$

Here the norms are just the Euclidean norms for the three dimensional complex vectors.

The above steps provide the general way to obtain the parameters using the inverse scattering algorithm. However, if the velocity of the rotating objects are small enough, then we may adopt a two-step procedure for the inversion. Since the contribution to the fields due to the rotation will be small, the media may be assumed to be at rest for reconstruction the geometric and dielectric data. Thus the cost function for this step will be as follows.

$$CF_1(\mathbf{u}, \mathbf{u}_1^{trial}) = \frac{\sum_{s=1}^S \sum_{m=1}^M \|\mathbf{E}^{fsp,rest}(s, m, \mathbf{u}_1^{trial}) - \mathbf{E}^{meas}(s, m, \mathbf{u})\|_{l2}^2}{\sum_{s=1}^S \sum_{m=1}^M \|\mathbf{E}^{meas}(s, m, \mathbf{u})\|_{l2}^2} + \frac{\sum_{s=1}^S \sum_{m=1}^M \|\mathbf{H}^{fsp,rest}(s, m, \mathbf{u}_1^{trial}) - \mathbf{H}^{meas}(s, m, \mathbf{u})\|_{l2}^2}{\sum_{s=1}^S \sum_{m=1}^M \|\mathbf{H}^{meas}(s, m, \mathbf{u})\|_{l2}^2} \quad (2)$$

Here the vector $\mathbf{u}_1^{trial} = (\mathbf{u}_g^{trial}, \mathbf{u}_d^{trial})$ contains the geometric and dielectric unknowns and the fields are calculated with the analytic solver for the rest case.

In the second step, we estimate the velocity by optimizing the following cost function that uses forward scattering procedure for the rotating media along with the approximate geometric and dielectric data \mathbf{u}_1^{as} obtained from the previous step.

$$CF_2(\mathbf{u}, \mathbf{u}_1^{as}, \mathbf{u}_v^{trial}) = \frac{\sum_{s=1}^S \sum_{m=1}^M \|\mathbf{E}^{fsp}(s, m, \mathbf{u}_1^{as}, \mathbf{u}_v^{trial}) - \mathbf{E}^{meas}(s, m, \mathbf{u}_v)\|_{l2}^2}{\sum_{s=1}^S \sum_{m=1}^M \|\mathbf{E}^{meas}(s, m, \mathbf{u}_v)\|_{l2}^2} + \frac{\sum_{s=1}^S \sum_{m=1}^M \|\mathbf{H}^{fsp}(s, m, \mathbf{u}_1^{as}, \mathbf{u}_v^{trial}) - \mathbf{H}^{meas}(s, m, \mathbf{u}_v)\|_{l2}^2}{\sum_{s=1}^S \sum_{m=1}^M \|\mathbf{H}^{meas}(s, m, \mathbf{u}_v)\|_{l2}^2} \quad (3)$$

Both these steps are much simpler than using the cost function in (1). For the first step, the forward scattering procedure is much simpler due to the lack of motion and the optimization is also simpler because the unknowns related to the velocity are not present. The second step is simpler as well, because it just requires the optimization for just the velocity parameters. Since the complexity of the optimization increases much faster than linear, the two steps combined can be more efficient than doing the direct optimization of the full cost function.

For the optimization, we adopt the differential evolution (DE) algorithm [6]. DE is a meta-heuristic algorithm that starts with a random initial population of size N_p in the search space and keeps on improving the solution by introducing stochastic variations to the candidate solutions until a termination criteria is satisfied. Here the condition used for termination is that either the maximum number of iterations, N_{lim} is reached or the cost function does not improve more than by a factor of f_{conv} in N_{conv} consecutive iterations.

2 Numerical results

2.1 Comparison of two-step procedure with the general algorithm

In this section we provide some numerical results for the reconstruction of the speeds of rotating objects from the scattered electromagnetic fields. The simulations are performed on a Intel i7-8565U, 1.8GHz, 8 core machine with 16 GB RAM. We consider a simple configuration of a homogeneous sphere rotating at a uniform speed. A first order semi analytic solution for this problem is available in the literature for such a problem [4]. We analyze the performance of the general algorithm as well as that of the two-step procedure for the reconstruction of the speed.

A sphere of radius $R_s = 1$ m is considered which is rotating about the z axis at angular velocity ω_s rad/s and is illuminated by a single plane wave source ($S = 1$) incident along x axis with a frequency of $f_s = 50$ MHz. The incident electric field is polarized along z axis. The speed of rotation can be expressed in terms of the normalized quantity $\beta = \omega_s R_s / c_0$, where c_0 is the speed of light in vacuum. The results are for $\epsilon_r = 8$ and $\beta \in \{8 \cdot 10^{-3}, 8 \cdot 10^{-4}, 8 \cdot 10^{-5}\}$ and are calculated at $M = 200$ points uniformly distributed on a circle on xz plane of radius $R_m = 1.5$

Rotating speed	Algorithm	Mean relative errors		Mean number of iterations	Mean number of function evaluations	Mean minimum cost	Mean time of simulation (seconds)
		ε_r	β				
$\beta = 8 \cdot 10^{-3}$	General algorithm	$1.39 \cdot 10^{-4}$	$4.67 \cdot 10^{-3}$	40.75	427.50	$3.14 \cdot 10^{-4}$	7398.0
	Two-step procedure	$1.12 \cdot 10^{-4}$	$2.66 \cdot 10^{-3}$	16.00 19.50	180.00 215.00	$9.62 \cdot 10^{-3}$ $3.04 \cdot 10^{-4}$	1511.1 3037.8
$\beta = 8 \cdot 10^{-4}$	General algorithm	$1.79 \cdot 10^{-4}$	$1.34 \cdot 10^{-1}$	33.50	355.00	$3.16 \cdot 10^{-4}$	6462.8
	Two-step procedure	$3.74 \cdot 10^{-5}$	$2.54 \cdot 10^{-2}$	19.25 19.50	212.50 215.00	$3.98 \cdot 10^{-4}$ $3.04 \cdot 10^{-4}$	1332.0 3595.3
$\beta = 8 \cdot 10^{-5}$	General algorithm	$3.05 \cdot 10^{-2}$	$1.49 \cdot 10^2$	20.25	222.50	$1.00 \cdot 10^{-1}$	3419.5
	Two-step procedure	$1.75 \cdot 10^{-4}$	$3.43 \cdot 10^{-1}$	17.50 19.25	185.00 212.50	$3.16 \cdot 10^{-4}$ $3.11 \cdot 10^{-4}$	1607.0 2993.3

Table 1: Comparison of general algorithm to the two-step procedure for the reconstruction of the rotating speed of sphere. The data is for an SNR level of 40 dB in each component of the measured data. The sphere is of radius $R_s = 1$ m, incident field is of $f_s = 50$ MHz frequency incident perpendicular to the axis of rotation. The actual value of ε_r is 8. Three values of the speeds β are considered and the results are averaged over four test runs.

m from the center of the scatterer. The electric and magnetic fields thus obtained are corrupted with a Gaussian noise of specified signal to noise ratio (SNR). We consider SNR dB levels in the set $\{20, 30, 40, 50, 60\}$ added to each component of the electric and magnetic fields.

The inversion is carried with the DE algorithm with a population size of $N_p = 10$. The parameters related to the termination of the algorithm are set as $N_{lim} = 100$, $f_{conv} = 0.01$ and $N_{conv} = 10$. The range over which the solutions are searched for is $\varepsilon_r \in (1, 20)$ and $\beta \in (-1, 1)$.

Table 1 summarizes the results for the case when $\text{SNR} = 40$ dB for three different values of β which are in the set $\{8 \cdot 10^{-3}, 8 \cdot 10^{-4}, 8 \cdot 10^{-5}\}$. The general algorithm tries to find both the unknowns together using the DE algorithm with the cost function in (1) and with $\mathbf{u} = (\varepsilon_r, \beta)$. As described in the previous section, the two-step procedure first tries to find the solution for $\mathbf{u}_1 = \varepsilon_r$ by minimizing the cost function in (2) by ignoring any rotation of the media. The approximate solution thus found in the first step is then used in the second step to solve for the value of $\mathbf{u}_2 = \beta$ by minimizing the cost function in (3).

Considering the stochastic nature of the optimization algorithm, all the results are averaged over four test runs for each configuration. As can be seen from the table, for $\text{SNR} = 40$ dB, both the algorithms give good results when the value of $\beta = 8 \cdot 10^{-3}$. The relative errors in ε_r are 0.0139 percent and 0.0112 percent for the general algorithm and the two-step procedure respectively. The corresponding relative errors in β are 0.467 percent and 0.266 percent. However, the two-step procedure is able to find the solution in 1 hour and 15 minutes where as the general algorithm took 2 hour and 3 minutes to find the solution. The performance of the two-step procedures improves relative to the general procedure when the rotating speeds are lower. For $\beta = 8 \cdot 10^{-4}$, the two-step procedure obtains the solutions for ε_r and β with relative errors of 0.00374 percent and 2.54 percent respectively. The corresponding relative errors in the solution obtained from the general algorithm are 0.0179 percent and 13.4 percent. Finally when $\beta = 8 \cdot 10^{-5}$, the general algorithm give completely unreliable result for β while the two-step procedure gives a value with 34.3 percent relative error.

In conclusion, the two-step procedure provides more accurate solutions than the general algorithm as the rotating speed gets lower. The time of simulation is much lower for the two-step procedure than the general algorithm. The solutions are reliable for lower values of speeds as long as the noise level is not too high.

To better understand how the results are affected by the noise we give the effect of SNR values on the error. In Figure 1 the mean relative error in the reconstructed value of β is plotted against the SNR levels in dB. The plots for three rotating speeds, $\beta \in \{8 \cdot 10^{-3}, 8 \cdot 10^{-4}, 8 \cdot 10^{-5}\}$, are shown. For $\beta = 8 \cdot 10^{-3}$, the relative error is just 0.032 percent for SNR = 60 dB and it increases to 8.2 percent when SNR = 20 dB. When $\beta = 8 \cdot 10^{-4}$, the average relative error values are 0.35 percent for SNR = 60 dB and 27 percent for SNR = 20 dB. Finally, for $\beta = 8 \cdot 10^{-5}$, the average relative errors are 4.47 percent for SNR = 60 dB and 493.6 percent for SNR = 20 dB. Thus the solutions are acceptable when the rotating speed is not too low and the noise level is not too high. But for small values of rotating speed, we need better and better precision in the measurement of the fields to get reliable result using the inversion procedure.

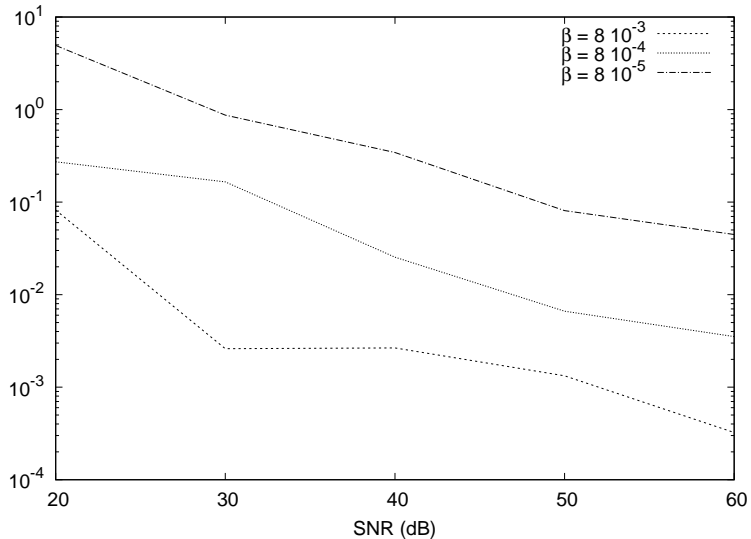


Figure 1: The mean relative error in the reconstructed value of β vs the SNR levels in dB for the rotating sphere. The results are shown for three different values of β .

2.2 Performance of two-step procedure with simpler sensors

In the previous subsection we examined the performance of the reconstruction algorithm when the measurement of the complex fields was available on the full circle outside the scatterer. Now we examine the performance of the second step of the two-step algorithm under limitations introduced by the sensors. First we study the effect of restricting the measurement points to only a small portion along the backscattering direction. After that we also investigate the effect of having only the amplitude data for the electromagnetic fields which can allow us to use much simpler sensors.

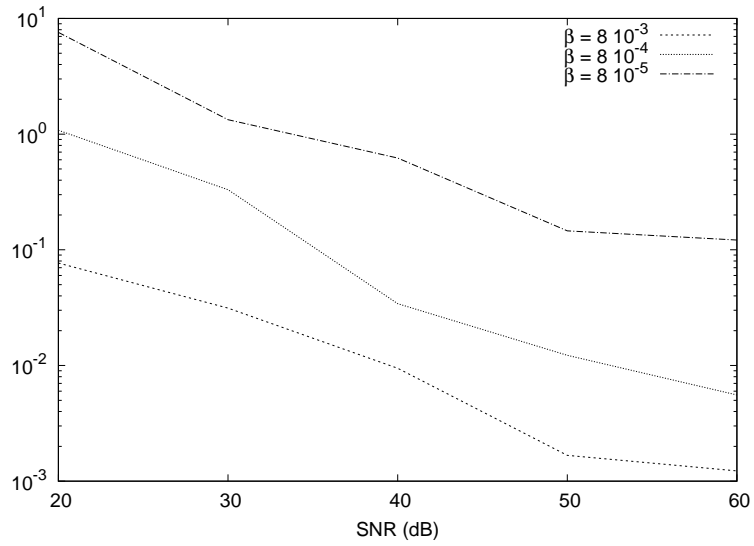


Figure 2: The mean relative error in the reconstructed value of β vs the SNR levels in dB for the rotating sphere using data in the back scattered direction. The results are shown for three different values of β .

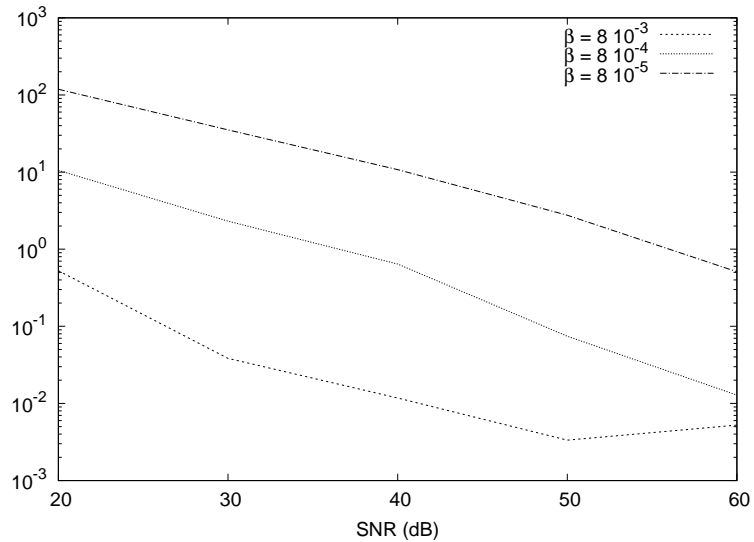


Figure 3: The mean relative error in the reconstructed absolute value of β vs the SNR levels in dB for the rotating sphere using amplitude only data in the back scattered direction. The results are shown for three different values of β .

The results for considering only the measurement point along the backscattered direction are provided in Figure 2. For this we use only the portion of measurement data that belongs to an arc subtending an angle of 90 degrees along the back scattering direction. So we considered 50 measurement points on an arc on xz plane of radius 1.5 m from the center of the scatterer. It is

observed that the reconstruction algorithm still works well with such a restriction. For example for $\beta = 8 \cdot 10^{-4}$ and with SNR = 60 dB, the relative error in the reconstructed value of β is 0.55 percent as compared to 0.35 percent obtained previously using the data on the full circle. For $\beta = 8 \cdot 10^{-4}$ and SNR = 40 dB, the corresponding values are 3.4 percent and 2.5 percent. With $\beta = 8 \cdot 10^{-4}$ and SNR = 20 dB the errors become 108.1 percent using the data along back scattered direction as opposed to 27.3 percent with the data on the full circle.

Next we examine the effect of using sensors that can measure only the amplitude of the electromagnetic fields. For this case we have to modify the cost functions involved so that only differences in the magnitudes of each components of the fields are considered. The measurement points used for the reconstruction are the same as those in the previous step involving only back scattered fields. In this case it is not possible to distinguish between the clockwise and anticlockwise rotations and therefore we have to consider only the absolute value of the reconstructed β . The results are provided in Figure 3. As expected, the accuracy is not as good as the results obtained with both amplitude and phase information. For example, with $\beta = 8 \cdot 10^{-4}$ and with SNR = 40 dB, the error in the reconstructed speed is 64.1 percent as opposed to 3.4 percent error obtained using both amplitude and phase measurements. However, with less noisy data the accuracy is acceptable as in the case with $\beta = 8 \cdot 10^{-4}$ and with SNR = 60 dB, where we get an error in the reconstructed speed of 1.28 percent. Similar comparisons can be made for the case of $\beta = 8 \cdot 10^{-3}$ and $\beta = 8 \cdot 10^{-5}$ shown in the figures and the results are good when the speed is not very small and the SNR is good enough.

Therefore in conclusion, we still get good solutions for the rotating speeds when the measurement is restricted to the back scattering direction. The results are degraded when only amplitude data is available but the errors are still small when the speeds are not too small and the noise is not too high.

2.3 Reconstruction of the speed of rotation from far-field data

So far, we concentrated on the performance of the reconstruction algorithm using the total field data in the near-field region. Next, let us analyze the performance of the algorithm with the scattered electromagnetic field in the far-field region. For this we consider the measurement arc on xz plane in the backscattered direction of radius $1.5 \cdot 10^3$ m from the center of the scatterer. The results are plotted in Figure 4.

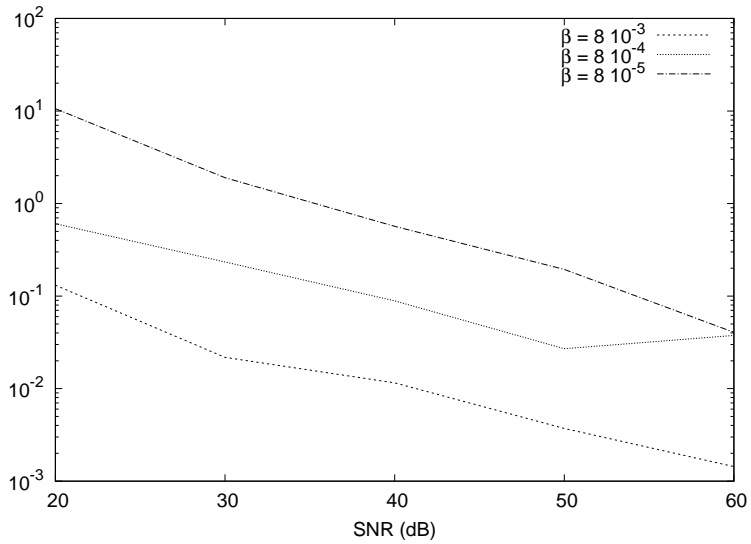


Figure 4: The mean relative error in the reconstructed value of β vs the SNR levels in dB for the rotating sphere using far-field data in the back scattered direction. The results are shown for three different values of β .

The algorithm performs well for $\beta = 8 \cdot 10^{-3}$ and the error for SNR values greater than or equal to 30 dB is less than 2.2 percent and is 13.1 percent for SNR of 20 dB. However, for $\beta = 8 \cdot 10^{-4}$, the error in the reconstructed value of β is 3.7 percent for SNR of 60 dB and is around 9 percent for 40 dB and rises to 23 percent for 30 dB SNR. Finally, for $\beta = 8 \cdot 10^{-5}$, the reconstruction algorithm performs very poorly. The error for 60 dB SNR in the data is 4 percent while for 50 dB the error is 19.3 percent and rises to unacceptable levels as the noise increases.

Let us also examine the effect of error in the knowledge of the axis of rotation of the scatterer. For this we may generate the measurement data using the forward model on an arc whose plane is rotated by some degree α from the xz plane while still using the old set of points for the reconstruction algorithm. The results with such an approach is shown in Figure 5 for $\alpha = 10^\circ$. For $\beta = 8 \cdot 10^3$, the algorithm is able to find the value of the rotating speed with an error of less than 1.6 percent for SNR values greater than or equal to 30 dB. The error for $\beta = 8 \cdot 10^{-4}$ is 1.3 percent for SNR of 60 dB, 15.1 percent for SNR of 40 dB SNR and 22.8 percent for SNR of 30 dB. Finally, for $\beta = 8 \cdot 10^{-5}$, the results are unreliable with a 36 percent error even for SNR of 60 dB, which rises to 102 percent error for SNR of 40 dB.

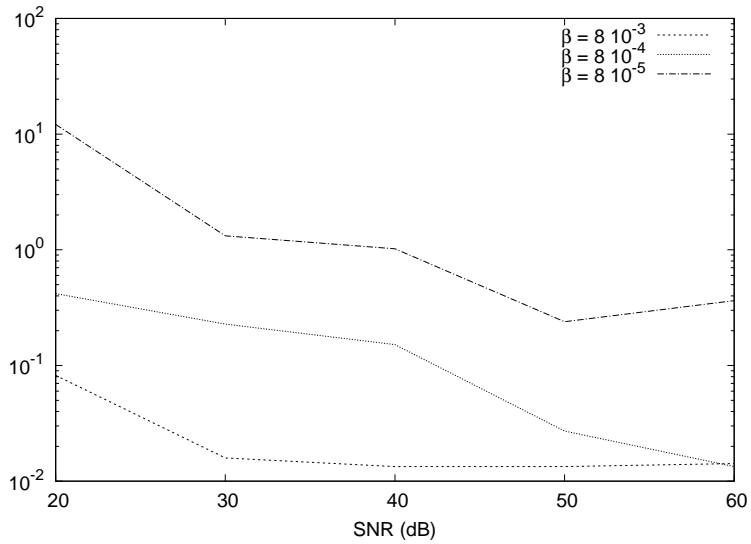


Figure 5: The mean relative error in the reconstructed value of β vs the SNR levels in dB for the rotating sphere using far-field data in the back scattered direction and $\alpha = 10^\circ$. The results are shown for three different values of β .

2.4 Reconstruction of the speed of rotating torus

All the previous results were obtained for rotating sphere which admitted a semi analytic solution for the forward problem. Now we apply the algorithm to rotating homogeneous torus for which analytic solutions are not available, due to which a numerical forward solver has to be exploited. The direct solution for the fields is obtained using a finite element method [7], [5]. The solver is implemented using a model in the commercial simulator COMSOL Multiphysics (COMSOL, Burlington, MA). The axis of symmetry of the torus is taken as z axis about which the torus rotates with an angular velocity of ω_s . The major radius, R_{tor} , and the minor radius, r_{tor} , of the torus [5] are taken as respectively 0.75 m and 0.25 m. We may express the speed of rotation using the normalized quantity $\beta = \frac{\omega_s(R_{tor}+r_{tor})}{c_0}$. The scattering medium is characterized by $\epsilon_r = 8$ and $\mu_r = 1$. It is illuminated by a plane wave incident along the x axis, polarized along z axis and with a frequency $f_s = 150$ MHz.

The numerical domain is set to $R_d = 4$ m and the measurement data are taken at $M = 200$ uniformly placed points on a circle in xz plane of radius $R_m = 1.5$ m. The variational formulation is implemented in the mathematics module of the COMSOL Multiphysics using a second order edge element formulation. A tetrahedral meshing is done with 241181 elements, 41605 nodes and 9438 boundary elements. The algebraic solver used is GMRES with a tolerance of 10^{-4} and with geometric multigrid preconditioner. The reconstruction algorithm searches for the optimal value of β in the range $(0, 10^{-2})$ and the parameters of the DE optimizer are same as before ($N_p = 10$, $N_{lim} = 100$, $f_{conv} = 0.01$, $N_{conv} = 10$). The measured data is corrupted with noise as before with SNR levels varying from 20 dB to 60 dB. Compared to the analytical solutions, the numerical solvers produce additional noise in the form of discretization errors and the tolerance in algebraic solver which could affect the performance of the inverse algorithm.

The results are shown in Figure 6 for values of $\beta \in \{8 \cdot 10^{-3}, 8 \cdot 10^{-4}, 8 \cdot 10^{-5}\}$. For $\beta = 8 \cdot 10^{-3}$, the relative error in the solution is less than 1.6 percent when SNR in the measured data is greater than or equal to 30 dB. In the case of $\beta = 8 \cdot 10^{-4}$, the relative errors are 2.14 percent for

50 dB SNR, 13.9 percent for 40 dB SNR and 21.6 percent for 30 dB SNR. When $\beta = 8 \cdot 10^{-5}$, the relative errors are very high. It is 16.7 percent for 60 dB SNR, 29.9 percent for 50 dB SNR and more than 100 percent when SNR is greater than or equal to 40 dB. As mentioned before, the additional noise in the numerical solver is a reason for the worse performance of the reconstruction algorithm compared to the case with semi analytic forward solver.

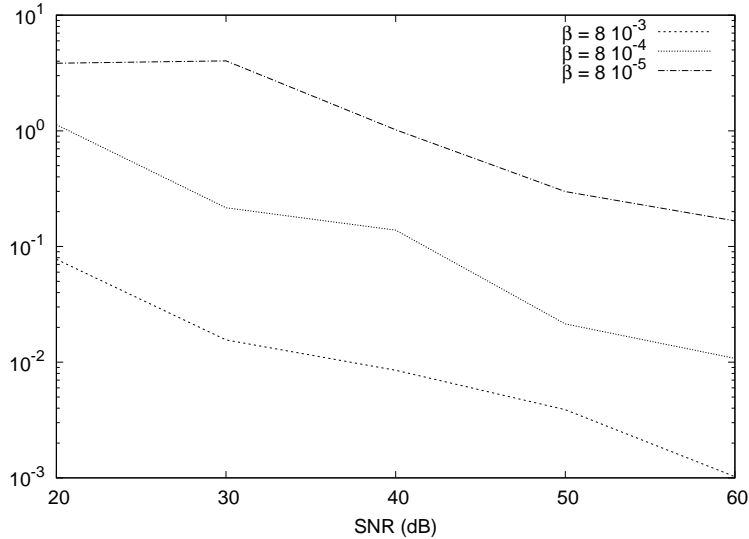


Figure 6: The mean relative error in the reconstructed value of β vs the SNR levels in dB for the rotating torus with measurement data on a circle of radius $R_m = 1.5$ m on the xz plane. The results are shown for three different values of β .

References

- [1] M. Pastorino, M. Raffetto, and A. Randazzo, “Electromagnetic inverse scattering of axially moving cylindrical targets,” *IEEE Transactions on Geoscience and Remote Sensing*, vol. 53, no. 3, pp. 1452–1462, March 2015.
- [2] M. Brignone, G. L. Gragnani, M. Pastorino, M. Raffetto, and A. Randazzo, “Noise limitations on the recovery of average values of velocity profiles in pipelines by simple imaging systems,” *IEEE Geoscience and Remote Sensing Letters*, vol. 13, no. 9, pp. 1340–1344, 2016.
- [3] J. G. V. Bladel, *Electromagnetic Fields*, 2nd ed. Piscataway, NJ, USA: IEEE Press, 2007.
- [4] D. D. Zutter, “Scattering by a rotating dielectric sphere,” *IEEE Transactions on Antennas and Propagation*, vol. 28, no. 5, pp. 643–651, September 1980.
- [5] P. Kalarickel Ramakrishnan and M. Raffetto, “Well posedness and finite element approximability of three-dimensional time-harmonic electromagnetic problems involving rotating axisymmetric objects,” *Symmetry*, vol. 12, no. 2, p. 218, 2020.
- [6] R. Storn and K. Price, “Differential evolution—a simple and efficient heuristic for global optimization over continuous spaces,” *Journal of global optimization*, vol. 11, no. 4, pp. 341–359, 1997.

[7] J. Jin, *The finite element method in electromagnetics*. New York: John Wiley & Sons, 1993.